Experimental study of AP–HTPB solid propellant combustion under periodic strain conditions

Mingming Gu[1*], Jianfeng Ouyang[1], Shaojie Wang[1], Xiaoming Shi[2], Kaiyu Hou[3], Zhongyue Zhou[1*], Fei Qi[1]
[1] School of Mechanical Engineering, Shanghai Jiao Tong University, Shanghai, 200240, China
[2] Shanghai Electro-Mechanical Engineering Institute, Shanghai 201109, China
[3] Shanghai Academy of Spaceflight Technology, Shanghai 201109, China

1 Introduction

The combustion of solid propellant can provide tremendous thrust to drive solid rocket motors. Solid propellant grains are subjected to mechanical loads during practical combustion applications. The causes of mechanical loads include, but are not limited to, impulsive loads during ignition and periodic loads (>5 Hz) due to mechanical oscillation[1, 2]. Since the propellant is comprised of a high-volume fraction (60%–75%) of microscopic solid oxidizer particles that are bonded to an elastomeric matrix, mechanical loading causes interfacial debonding of the particles, which seriously affects the combustion behaviours of the propellant[3-9]. Therefore, investigating the transient combustion characteristics under strain condition is of great significance for understanding the complex combustion behaviour of solid propellants as well as improving the propellant combustion strategy[10].

Due to the harsh conditions of propellant combustion, the detection of the combustion characteristics such as temperature, burning rate, and combustion products is extremely challenging. Currently, in-situ measurement of gaseous combustion products such as CO_2, CO and H_2O etc. can be performed by nonintrusive spectroscopic methods[10-16]. Among those methods, laser absorption spectroscopy (LAS) [13-16] is capable of measuring the combustion temperature and combustion products simultaneously. Besides, for the measurement of propellant burning rate, high-speed photography [17, 18] shows advantages in identifying the real-time jitter of burning rates.

To facilitate optical diagnostics, many laboratory-scale combustion devices with optical access were reported for propellant combustion measurement[17-21], most of which can provide high-pressure conditions but not capable of exerting mechanical loadings onto the solid propellant. Recently, Hu et al. [22, 23] reported the measurement of the propellant burning rate variations under different static tensile loadings, they found that the burning rate of solid propellant would grow linearly with the relative strain when the extent of deformation was small (0-10%).

In this work, we designed and fabricated a high-pressure combustion apparatus that can provide mechanical loadings onto solid propellant and have windows access for optical diagnostics. Combustion temperature, CO and CO_2 column densities were measured simultaneously through a LAS system, and

Correspondence to: zhongyue.zhou@sjtu.edu.cn

the propellant burning rate was obtained through high-speed photography. Both static and dynamic strain conditions were investigated and measurements were performed under different pressures.

2 Experimental Setup

The high-pressure combustion chamber was made of GB/T 45 medium carbon steel and the internal volume is approximately 2 L with a diameter of 130 mm and height of 100 mm. Two sapphire windows with a diameter of 50 mm and a thickness of 60 mm were mounted in window plugs located on opposite sides of the chamber (Figure 1(b)), providing a clear optical access with a diameter of 30 mm. The transmittance of 4-5 μm light emission for tandem windows exceeded 45%. The I-shaped propellant grain was placed in the middle of the two windows, allowing a laser beam to pass over. A pair of fixed and movable clamps were used to hold the grain, and the movable one was connected to a cylindrical shaft to reciprocate the compression and tension of the grains. For the ignition unit, a 15-mm length tungsten wire with a diameter of 0.2 mm was placed on the top of the grain and connected to a 1 W DC power supply via two copper feedthroughs.

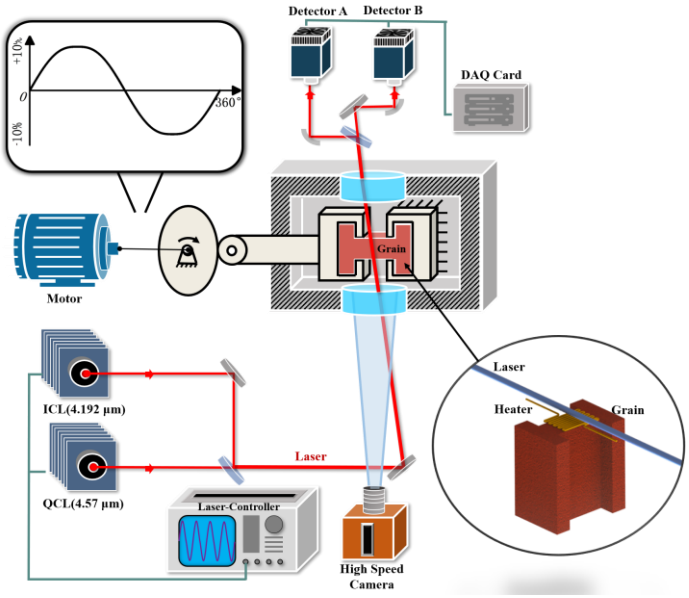

Figure 1. Schematic of the diagnostic system[24, 25]

Figure 1 shows a schematic of the diagnostic system. The measurement system mainly comprises a high-speed camera (Vision Research VEO340L) and a QCL with a center wavelength at 4.57 μm (Hamamatsu) as well as an ICL with a center wavelength of 4.192 μm (Nanoplus). For the high-speed imaging system, the camera took the propellant combustion at 4 kHz with a photo resolution of 0.0374 mm/pixel. Exposure time was set at 1 μs to avoid overexposure. While the camera shot, the LAS also started collecting data. A function generator (Tektronix AFG3022C) was used to generate two 10 kHz triangle waveforms that had the same phase but different voltage amplitudes to accommodate the operational voltages for QCL and ICL, respectively. The two lasers were first combined by a beam splitter (Rayan BSM5050) and then sent into the combustion chamber. The transmitted laser beam was spectrally separated by a barrow bandpass filter (Rayan BP4500), and the transmitted (4.57 μm) and were finally received by two thermoelectrically cooled mercury cadmium telluride (MCT) photovoltaic detectors (PUI-3TE, Vigo System). The absorption spectrums were obtained by the transmitted laser beams and the spectrums' wavelength was calibrated by a germanium etalon. The free spectral range (FSR) of the etalon was 0.014 cm^{-1} at 4.57 μm and 0.0127 cm^{-1} at 4.192 μm.

The aluminized AP-HTPB propellant consisted of 70 wt. % AP, 15 wt. % aluminum, and 15 wt. % binder, approximately. The propellant was burned in a specially designed combustion chamber which

could operate at pressures up to 15 MPa. The entire combustion chamber was properly sealed and purged with pure N_2 each time before and after the measurement. One side of the propellant grain was clamped by a fixed mount while the other side was clamped together with a movable shaft. The shaft could be fixed at a given position or moved periodic to provide strain to the propellant. The deformation of the solid propellant is characterized by the relative strain ε as

$$\varepsilon = \Delta\omega / \varpi \tag{1}$$

where ϖ and $\Delta\omega$ are the original (10 mm) and the change of the propellant length due to strain, respectively.

Before each measurement, the propellant was ignited by a thin heated wire displaced on the top center of the propellant surface (as shown in the inset of Figure 1). The high-speed camera has an image trigger function, and the camera would start shooting when the propellant was ignited. At the same time, the camera sent a trigger signal to the LAS system so that the two diagnostic methods were synchronized in time.

3 Results and Discussions

3.1 AP-HTPB combustion with static strain

Figure 2(a) shows an example of the measured propellant burning surface positions. Data measured within 500 ms and after 2000 ms were dropped because the propellant flame was unstable during these time periods. The burning rate could be calculated by fitting the flame surface position with a primary function. For three initial pressures (0.1 MPa, 0.2 MPa, and 0.5 MPa), the propellant burning rate was higher when the propellant was stretched ($\varepsilon = +10\%$) than when it was compressed ($\varepsilon = -10\%$) and was higher at high pressures. The uncertainty of burning rate were evaluated from the fitting process and can be seen in Figure 2(b). The boost of the propellant burning rate at higher relative strain conditions could be related to the enhancement of the gas permeability as well as the increase of the burning surface.

The LAS measurement results are shown in Figure 3. The shaded areas in Figs. 3(a-c) represent the 95% confidence intervals for temperature, CO, and CO_2 column densities. According to the literature[21], in which the AP-HTPB flame was measured in a similar setup, the time-averaged flame temperature was 1926 K higher than in this work (1652 K). This discrepancy was likely due to the heat loss when the combustion product reached the laser path.

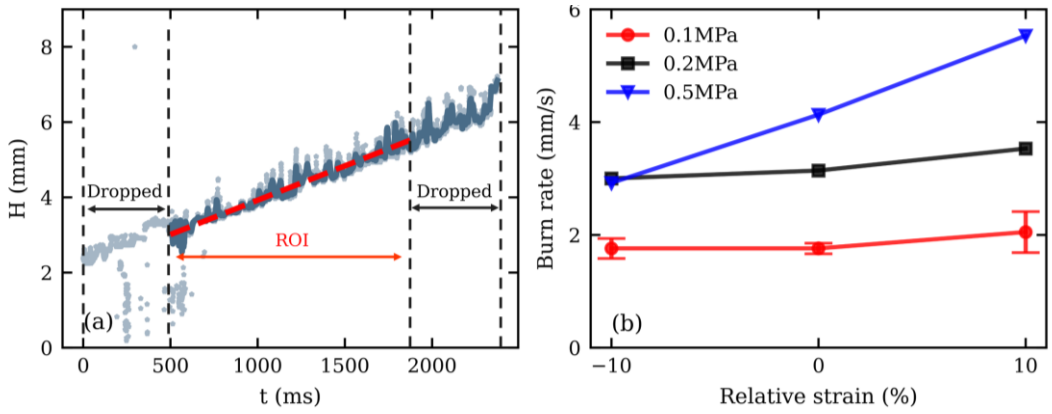

Figure 2. (a) AP-HTPB propellant burning surface positions at different times (0.1 MPa initial pressure and 0% relative strain). (b) Burning rate of AP-HTPB propellant at different initial pressures and different relative strains[25].

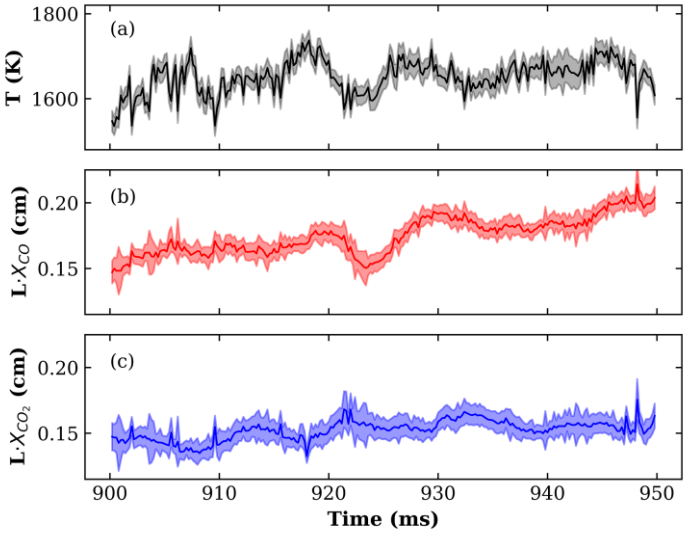

Figure 3. Time-resolved measurements of (a) flame temperature, (b) CO column density, and (c) CO_2 column densities. (0.1 MPa initial pressure and 0% relative strain)[25]

3.2 AP-HTPB combustion with cyclic loading

The propellant combustion process under cyclic loading was also measured, and the results are shown in Figure 4. The initial pressure of the chamber was at 0.1 MPa, and the frequency of the alternating strain was 24 Hz. Since the parameters measured by LAS change with sinusoids in time, a function in the form of $F(t) = Asin(2\pi f \cdot t + \varphi) + B$ was employed to reveal the relationships between these parameters and are displayed as dashed lines in Figure 4. The results showed that the propellant temperature, CO, and CO_2 column density also changed with the cyclic loading at a frequency of 24 Hz. Due to the interconversion relationship of CO and CO_2, their phase is delayed by $\pi/2$ than that of temperature.

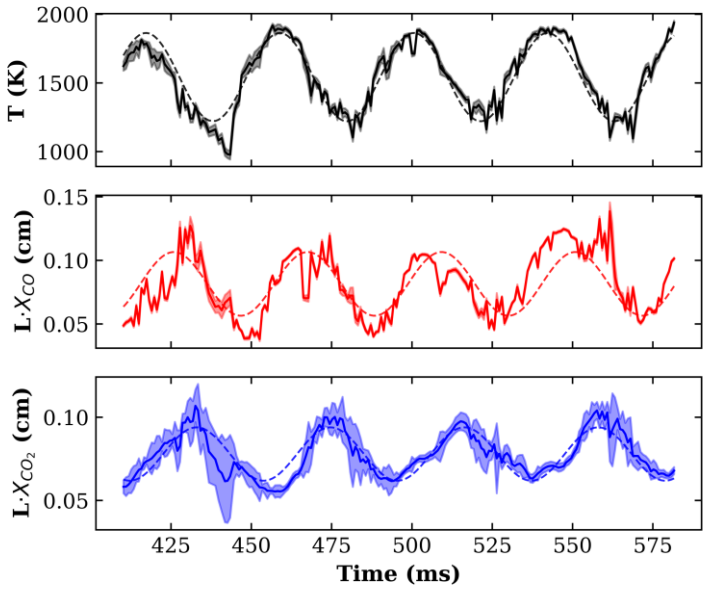

Figure 4. Best-fit (a) temperature, (b) CO, and (c) CO_2 column densities. (0.1 MPa initial pressure and ±10% relative strain.) The shaded areas denote the 95% confidence interval as form the spectral fitting routine[25]

4 Conclusions

In this work, we present the experimental measurement of temperature, CO and CO_2 species as well as the burning rate of aluminized AP-HTPB propellant combustion when different extend of relative strain was applied. We found that the propellant burning rate and the combustion temperature increased with higher relative strain, and this trned was more significant for burning rate and less evident for combustion temperature at higher pressures. The prilimary results presented in this work are of practcial interests to the propellant combustion studies. Future work will focus on the experimental measurements at extended pressure ranges. Besides, we aim to develop a detailed kinetic model that can account for the strain effects and to explain the resultant temperature and production composition variations as observed experimentally.

Acknowledgement

This work was supported by the National Natural Science Foundation of China (52206222).

References

1. Kurian, M.; Renganathan, K.; Sobichen, S. M., Structural analysis of viscoelastic solid propellant grain. *Int. J. Sci. Eng. Res.* **2016,** *7* (10), 117-122.
2. Wei, S. J.; Jin, B. N.; Liu, P. J. In *Parameters analysis of Non-linear combustion instability based on the pulsed trigger T-burner technique*, 9th International Conference on Mechanical and Aerospace Engineering (ICMAE), Budapest, Hungary, 2018 Jul 10-13; Budapest, Hungary, 2018; pp 531-535.
3. Bentil, S. A.; Jackson, W. J.; Williams, C.; Miller, T. C., Viscoelastic properties of inert solid rocket propellants exposed to a shock wave. *Propellants, Explosives, Pyrotechnics* **2021,** *46*, 1-16.
4. Li, J. X.; Mo, W. B.; Tang, J. L., Research on mechanical property prediction of solid propellant base on GA-BP neural network. *Comput. Simul.* **2011,** *28* (1), 76-79.
5. Ozupek, S.; Becker, E. B., Constitutive equations for solid propellants. *J. Eng. Mater. Technol.* **1997,** *119* (2), 125-132.
6. Chaturvedi, S.; Dave, P. N., Solid propellants: AP/HTPB composite propellants. *Arabian J. Chem.* **2019,** *12*, 2061-2068.
7. Bencher, C. D.; Dauskardt, R. H.; Titchie, R. O., Microstructural damage and fracture processes in a composite solid rocket propellant. *J. Spacecr. Rockets* **1995,** *32* (2), 328-334.
8. Tormey, J. F.; Britton, S. C., Effect of cyclic loading on solid propellant grain structures. *AIAA J.* **2015,** *1* (8), 1763-1770.
9. Koreki, T.; Aoki, I.; Shirota, K.; Toda, Y.; Kuratani, K., Experimental study on oscillatory combustion in solid-propellant motors. *J. Spacecr. Rockets* **2015,** *13* (9), 534-539.
10. Stufflebeam, J. H.; Eckbreth, A. C., CARS diagnostics of solid propellant combustion at elevated pressure. *Combust. Sci. Technol.* **1989,** *66*, 163-179.
11. Edwards, T.; Weaver, D. P.; Campbell, D. H.; Hulsizer, S., Investigation of high pressure solid propellant combustion chemistryusing emission spectroscopy. *J. Propul. Power* **1971,** *2* (3), 228-234.

12. Kearney, S. P.; Guildenbecher, D. R., Temperature measurements in metalized propellant combustion using hybrid fs/ps coherent anti-Stokes Raman scattering. *Appl. Opt.* **2016,** *55* (18), 4958-4966.
13. Yao, Z. P.; Zhang, W.; Wang, M.; Chen, J.; Shen, Y.; Wei, Y. M.; Yu, X. L.; Li, F.; Zeng, H., Tunable diode laser absorption spectroscopy measurements of high-pressure ammonium dinitramide combustion. *Aerosp. Sci. Technol.* **2015,** *45*, 140-149.
14. Guo, Y. P.; Li, J. M.; Gong, L.; Xiao, F.; Yang, R. J.; Meng, L. C., Effect of organic fluoride on combustion performance of HTPB propellants with different aluminum content. *Combust. Sci. Technol.* **2021,** *193* (4), 702-715.
15. Mathews, G. C.; Blaisdell, M. G.; Lemcherfi, A. I.; Slabaugh, C. D.; Goldenstein, C. S., High-bandwidth absorption-spectroscopy measurements of temperature, pressure, CO, and H_2O in the annulus of a rotating detonation rocket engine. *Appl. Phys. B* **2021,** *127* (12), 165-187.
16. Ruesch, M. D.; McDonald, A. J.; Mathews, G. C.; Son, S. F.; Goldenstein, C. S., Characterization of the influence of aluminum particle size on the temperature of composite-propellant flames using CO absorption and AlO emission spectroscopy. *Proceedings of the Combustion Institute* **2021,** *38* (3), 4365-4372.
17. Essel, J. T.; Boyer, E.; Kuo, K. K.; BaoGi, Z., Transient burning behavior of phase-stabilized ammonium nitrate based airbag propellant. *Int. J. Energ. Mater. Chem. Propul.* **2012,** *11* (5), 473-86.
18. Derk, G.; Risha, G. A.; Boyer, E.; Yetter, R. A., High-pressure burning rate measurements by direct observation. *Int. J. Energ. Mater. Chem. Propul.* **2019,** *18* (3), 213-227.
19. Mallery, C.; Kim, E.; Thynell, S. T., High-pressure strand burner system for propellant flame studies using absorption spectroscopy. *Rev. Sci. Instrum.* **1995,** *66* (8), 4091-4.
20. Tancin, R. J.; Mathews, G. C.; Goldenstein, C. S., Design and application of a high-pressure combustion chamber for studying propellant flames with laser diagnostics. *Rev. Sci. Instrum.* **2019,** *90* (4), 045111.
21. Tancin, R. J.; Chang, Z.; Radhakrishna, V.; Gu, M. M.; Goldenstein, C. S. In *Ultrafast Laser Absorption Spectroscopy in the Mid-Infrared for Measuring Temperature and Species in Combustion Gases*, AIAA Scitech 2020 Forum, 2020.
22. Hu, S. Q.; Deng, Z.; Liu, Y. J., Experimental research on burning rate change of composite propellant under strain. *J. Solid Rocket Technol.* **2013,** *36* (2), 230-233.
23. Hu, S. Q.; Chen, J.; Deng, Z.; Liu, Y. J., Computational analysis on burning rate change of composite propellant under tensile strain. *J. Solid Rocket Technol.* **2014,** *37* (5), 672-677, 683.
24. Ouyang, J. F.; Gu, M. M.; Wang, S. J.; Cui, C. H.; Shi, X. M.; Hou, K. Y.; Zhou, Z. Y.; Qi, F., A novel optical high-pressure apparatus for studying the combustion of solid propellant under periodic strain. *Sci. China: Technol. Sci.* **2022**.
25. Gu, M. M.; Ouyang, J. F.; Wang, S. J.; Yuan, W. H.; Shi, X. M.; Xiao, L. B.; Gao, H. X.; Zhou, Z. Y.; Qi, F., AP–HTPB propellant combustion under strain conditions with laser absorption spectroscopy. *Appl. Opt.* **2023,** *62* (6), A37-A45.